Physics Letters A 378 (2014) 2915–2923

Contents lists available at ScienceDirect

Physics Letters A

www.elsevier.com/locate/pla

Tachyonic Cherenkov radiation in the absorptive aether

Roman Tomaschitz

Department of Physics, Hiroshima University, 1-3-1 Kagami-yama, Higashi-Hiroshima 739-8526, Japan

ARTICLE INFO

Article history:
Received 21 July 2014
Received in revised form 10 August 2014
Accepted 11 August 2014
Available online 13 August 2014
Communicated by V.M. Agranovich

Keywords:
Tachyonic radiation fields
Complex permeability tensors and tachyon mass
Energy dissipation in a permeable spacetime
Green functions of dispersive Maxwell–Proca fields
Dissipative Cherenkov flux densities
Shock-heated plasma of supernova remnants

ABSTRACT

Dissipative tachyonic Cherenkov densities are derived and tested by performing a spectral fit to the γ-ray flux of supernova remnant (SNR) RX J1713.7 − 3946, measured over five frequency decades up to 100 TeV. The manifestly covariant formalism of tachyonic Maxwell–Proca radiation fields is developed in the spacetime aether, starting with the complex Lagrangian coupled to dispersive and dissipative permeability tensors. The spectral energy and flux densities of the radiation field are extracted by time averaging, the energy conservation law is derived, and the energy dissipation caused by the complex frequency-dependent permeabilities of the aether is quantified. The tachyonic mass-square in the field equations gives rise to transversally/longitudinally propagating flux components, with differing attenuation lengths determined by the imaginary part of the transversal/longitudinal dispersion relation. The spectral fit is performed with the classical tachyonic Cherenkov flux radiated by the shell-shocked electron plasma of SNR RX J1713.7 − 3946, exhibiting subexponential spectral decay.

1. Introduction

Decay is inherent in all composite matter, and the spacetime structure employed in physical modeling should reflect this fact. Here, we consider tachyonic wave propagation in a dissipative spacetime, the physical manifestation of the all-pervading aether. The aim is to quantify the effect of absorption on the spectral decay of radiation densities, to develop the general formalism and work out a specific example, dissipative tachyonic Cherenkov radiation [1–9], and to probe the decaying energy flux by performing a spectral fit to the γ-ray emission from an ultra-relativistic plasma. For the latter, we consider the shock-heated electron population of a supernova remnant.

To this end, we start with the complex Lagrangian of a Maxwell–Proca field coupled to dissipative permeability tensors, manifestly covariantly in a frequency-space representation. In contrast to non-dissipative real permeabilities, the complex dispersion relations unambiguously determine the retarded/advanced Green function without epsilon regularization. We derive the energy conservation law for the dissipating radiation field, and identify the spectral densities of field energy and Poynting vector by time averaging. In this way, we can also quantify the energy absorption induced by the complex permeabilities and the complex tachyonic mass-square in the field equations. The attenuation lengths defining the damping factor in the classical tachyonic Cherenkov densities differ for transversal and longitudinal radiation. We average these densities over a relativistic electron gas and put them to test by performing a spectral fit to the supernova remnant RX J1713.7 − 3946, whose γ-ray flux has been measured by the Fermi satellite [10] and the ground-based atmospheric imaging array HESS [11,12]. The spectral fit covers five frequency decades, the GeV range up to 100 TeV.

In Section 2, we introduce the tachyonic Maxwell–Proca Lagrangian in the absorptive spacetime aether described by complex frequency-dependent permeability tensors. We explain the meaning of the complex Lagrangian and the manifestly covariant action functional, and derive the field equations and the constitutive relations, manifestly covariantly and also in 3D. In Section 3, we derive the continuity equation for the field energy in the aether defined by homogeneous and isotropic permeabilities, and extract the spectral energy flux by time averaging. In Section 4, we separate the transversal and longitudinal components of the tachyonic radiation field to obtain explicit formulas for the dissipating transversal/longitudinal energy and flux densities.

In Section 5, we derive the dispersion relations from the wave equations for the transversal and longitudinal vector potentials, as well as asymptotic formulas for the complex transversal/longitudinal wavenumbers by ascending series expansion in the imaginary parts of the permeabilities. In Section 6, we discuss spherical

E-mail address: tom@geminga.org.

http://dx.doi.org/10.1016/j.physleta.2014.08.010
0375-9601/

wave propagation in the aether, employing transversal/longitudinal Green functions in space-frequency representation. In contrast to a non-absorptive spacetime, the Green function, retarded or advanced, is already determined by the imaginary part of the dispersion relation, without the use of epsilon regularization of pole singularities prescribing residual integration paths. We use the retarded Green function in dipole approximation to obtain the attenuated radiation fields at large distance from the localized source.

In Section 7, we calculate the classical tachyonic Cherenkov densities of an inertial subluminal charge in the dissipative aether. There are two different ways to derive the Cherenkov effect. In Fermi's approach, one considers the radiating charge moving along an infinite straight line, solves the field equations in cylindrical coordinates, and calculates the flux streaming orthogonally through a cylinder around the particle trajectory [3,4]. A preferable method due to Tamm is to consider the trajectory within a finite time interval, so that the current distribution is compact. The time-averaged asymptotic flux through a large sphere is then calculated in dipole approximation, and the averaging period is finally extended to infinity to remove the bremsstrahlung contribution occurring at the end points of the truncated trajectory [13,14]. This bremsstrahlung vanishes with increasing averaging period and is not to be confused with photonic bremsstrahlung which can arise in the weakly coupled plasma of the remnant [15–17]. The asymptotic spherical symmetry of Tamm's method is better adapted to the radiation problem studied here than an infinite cylindrical geometry. In Section 8, we average the transversal/longitudinal radiation densities over an ultra-relativistic thermal electron gas and perform a tachyonic Cherenkov fit to the γ-ray emission of SNR RX J1713.7 − 3946. In Section 9, we present our conclusions.

2. Maxwell–Proca Lagrangian in an absorptive spacetime

Throughout this article, we use a frequency-space representation of the real Proca field $\hat{A}_\mu(\mathbf{x},\omega) = \int_{-\infty}^{\infty} A_\mu(\mathbf{x},t)\mathrm{e}^{\mathrm{i}\omega t}\mathrm{d}t$, suitable for dispersive and dissipative permeabilities [18–21]. Time Fourier transforms are denoted by a hat, and the reality condition is $\hat{A}^*_\mu(\mathbf{x},\omega) = \hat{A}_\mu(\mathbf{x},-\omega)$. We start with the formally manifestly covariant Maxwell–Proca Lagrangian

$$\hat{L} = -\frac{1}{4}\hat{F}^*_{\mu\nu} g_F^{\mu\alpha} g_F^{\nu\beta} \hat{F}_{\alpha\beta} + \frac{1}{2} m_\mathrm{t}^2 \hat{A}^*_\mu g_A^{\mu\nu} \hat{A}_\nu + \frac{1}{2}\left(\hat{A}^*_\mu g_J^{\mu\nu} \hat{j}_\nu + \hat{A}_\mu g_J^{\mu\nu} \hat{j}^*_\nu\right), \tag{2.1}$$

where $\hat{F}_{\mu\nu}(\mathbf{x},\omega)$ is the Fourier transform of the field tensor $F_{\mu\nu} = A_{\nu,\mu} - A_{\mu,\nu}$. Time differentiation in Fourier space means to multiply with a factor $-\mathrm{i}\omega$, e.g. $\hat{A}_{\mu,0} = -\mathrm{i}\omega\hat{A}_\mu$ and $\hat{A}^*_{\mu,0} = \mathrm{i}\omega\hat{A}^*_\mu$ for conjugated fields. Greek indices are raised and lowered with the Minkowski metric $\eta_{\mu\nu} = \mathrm{diag}(-1,1,1,1)$. The permeability tensors $g^{\mu\nu}_{A,F,J}(\omega)$ are homogeneous and isotropic, satisfying the reality condition $g^{*\mu\nu}_{A,F,J}(\omega) = g^{\mu\nu}_{A,F,J}(-\omega)$ like the complex permeabilities $(\varepsilon_0(\omega), \mu_0(\omega))$, $(\varepsilon(\omega), \mu(\omega))$ and $\Omega(\omega)$ defining them,

$$g_A^{00} = -\varepsilon_0, \qquad g_A^{ij} = \frac{\delta^{ij}}{\mu_0},$$
$$g_F^{00} = -\mu^{1/2}\varepsilon, \qquad g_F^{ij} = \frac{\delta^{ij}}{\mu^{1/2}}, \tag{2.2}$$

and $g^{0i}_{A,F} = 0$. The tensor $g_J^{\mu\nu}(\omega) = \eta^{\mu\nu}/\Omega(\omega)$ is conformal to the Minkowski metric and amounts to a frequency-dependent coupling constant. All permeabilities have a positive real part, and principal values are assumed for roots. We use the Heaviside–Lorentz system, so that $\varepsilon = \varepsilon_0 = 1$ and $\mu = \mu_0 = 1$ in vacuum. The complex frequency-dependent tachyon mass $m_\mathrm{t}(\omega)$ in the Lagrangian satisfies $m_\mathrm{t}(-\omega) = m^*_\mathrm{t}(\omega)$, with positive real part. The mass-square can be scaled into $g_A^{\mu\nu}(\omega)$, cf. Section 3. The external current is conserved, $\hat{j}^\nu_{,\nu} = 0$ (that is $\hat{j}^m_{,m} - \mathrm{i}\omega\hat{j}^0 = 0$) and satisfies the reality condition. Lagrangian (2.1) is real only if the permeabilities and the tachyon mass are real, in the absence of absorption.

We define the inductive fields $\hat{H}^{\alpha\beta} = g_F^{\alpha\mu} g_F^{\beta\nu}\hat{F}_{\mu\nu}$ and $\hat{C}^\mu = g_A^{\mu\nu}\hat{A}_\nu$, as well as the dressed current $\hat{j}^\mu_\Omega = g_J^{\mu\nu}\hat{j}_\nu$, which are the manifestly covariant constitutive relations in the absolute spacetime. Euler variation of the Lagrangian with respect to $\hat{A}^*_\mu$ gives the field equations $\hat{H}^{\mu\nu}_{\ ,\nu} - m_\mathrm{t}^2\hat{C}^\mu = \hat{j}^\mu_\Omega$. Differentiation followed by contraction leads to the Lorentz condition $\hat{C}^\mu_{,\mu} = 0$, as the current is conserved. Variation of the Lagrangian with respect to $\hat{A}_\mu$ results in a different set of field equations, where the permeability tensors and the mass-square are replaced by the conjugated quantities, $g^{\mu\nu}_{A,F,J}(\omega) \to g^{*\mu\nu}_{A,F,J}(\omega)$, $m_\mathrm{t}(\omega) \to m^*_\mathrm{t}(\omega)$. The imaginary parts of the permeability tensors and the tachyon mass determine whether the Green function is retarded or advanced, cf. Sections 5.2 and 6.1. (In contrast to real permeabilities, there are no poles on the real axis to be circumvented by epsilon regularization, that is, by an infinitesimal $\pm\mathrm{sign}(\omega)\mathrm{i}\varepsilon$ or $\pm\mathrm{i}\varepsilon$ insertion in the denominator of the Green function in momentum space, cf. Section 6.) For any given frequency ω, either $(g^{\mu\nu}_{A,F,J}, m_\mathrm{t})$ or the conjugated quantities $(g^{*\mu\nu}_{A,F,J}, m^*_\mathrm{t})$ define retarded wave propagation, and we use the corresponding wave equation at this frequency. For the sake of definiteness, we will consider a frequency interval in which $(g^{\mu\nu}_{A,F,J}, m_\mathrm{t})$ gives retarded propagation.

If the permeability tensors and the tachyon mass are real and constant (frequency-independent), we can use a spacetime representation of the Lagrangian,

$$L = -\frac{1}{4}F_{\mu\nu}H^{\mu\nu} + \frac{1}{2}m_\mathrm{t}^2 A_\mu C^\mu + A_\mu j^\mu_\Omega, \tag{2.3}$$

resulting in the action $S = \int L\mathrm{d}\mathbf{x}\mathrm{d}t = (2\pi)^{-1}\int \hat{L}\mathrm{d}\mathbf{x}\mathrm{d}\omega$, with $\hat{L}$ in (2.1). In the case of complex frequency-dependent permeabilities, we employ the second identity to define the action. S is real since $\hat{L}(\mathbf{x},-\omega) = \hat{L}^*(\mathbf{x},\omega)$ and does not change if we replace Lagrangian (2.1) by its complex conjugate, which means to replace $(g^{\mu\nu}_{A,F,J}, m_\mathrm{t})$ by $(g^{*\mu\nu}_{A,F,J}, m^*_\mathrm{t})$.

The 3D field strengths are $\hat{E}_k = \hat{F}_{k0} = \mathrm{i}\omega A_k + A_{0,k}$ and $\hat{B}^k = \varepsilon^{kij}\hat{F}_{ij}/2 = \varepsilon^{kij}\hat{A}_{j,i}$, and inversely $\hat{F}_{ij} = \varepsilon_{ijk}\hat{B}^k$, where ε^{kij} is the Levi-Civita 3-tensor. The 3D inductions are defined by the constitutive relations $\hat{D}^l = \hat{H}^{0l} = \varepsilon\hat{E}^l$ and $\hat{H}_i = \varepsilon_{ikl}\hat{H}^{kl}/2 = \hat{B}_i/\mu$, as well as $\hat{C}_m = \hat{A}_m/\mu_0$ and $\hat{C}_0 = \varepsilon_0\hat{A}_0$ for the potential, cf. after (2.2). The charge densities $\hat{\rho} = \hat{j}^0$ and $\hat{\rho}_\Omega = \hat{j}^0_\Omega$ of external and dressed current are related by $\hat{\rho}_\Omega = \hat{\rho}/\Omega$, and the respective 3-currents by $\hat{j}^k_\Omega = \hat{j}^k/\Omega$. The 3D inhomogeneous field equations read

$$\varepsilon^{klj}\hat{H}_{j,l} + \mathrm{i}\omega\hat{D}^k - m_\mathrm{t}^2\hat{C}^k = \hat{j}^k_\Omega, \qquad \hat{D}^l_{,l} - m_\mathrm{t}^2\hat{C}^0 = \hat{j}^0_\Omega. \tag{2.4}$$

The homogeneous Maxwell equations follow from the above potential representation of the field strengths, and we also mention conservation of the dressed current and the Lorentz condition,

$$\varepsilon^{ikn}\hat{E}_{n,k} - \mathrm{i}\omega\hat{B}^i = 0, \qquad \hat{B}^i_{,i} = 0,$$
$$\mathrm{i}\omega\hat{j}^0_\Omega - \hat{j}^k_{\Omega,k} = 0, \qquad \mathrm{i}\omega\hat{C}^0 - \hat{C}^l_{,l} = 0. \tag{2.5}$$

The rising and lowering of the zero index is accompanied by a sign change, as we use the sign convention $\mathrm{diag}(-1,1,1,1)$ for the Minkowski metric.

3. Tachyonic Poynting vector and dissipative energy density

To derive the energy conservation law in an absorptive spacetime [22–25], we employ the inhomogeneous field equations (2.4), the homogeneous equations, current conservation and Lorentz condition in (2.5), as well as the constitutive relations stated before (2.4). We consider these equations at a fixed frequency ω and the conjugated equations at a different nearby frequency ω',

$$\varepsilon^{klj}\hat{H}^*_{j,l} - \mathrm{i}\omega'\hat{D}^{k*} - m_t^{2*}\hat{C}^{k*} = \hat{j}^{k*}_\Omega, \qquad \hat{D}^{l*}_{,l} - m_t^{2*}\hat{C}^{0*} = \hat{j}^{0*}_\Omega,$$
$$\varepsilon^{ikn}\hat{E}^*_{n,k} + \mathrm{i}\omega'\hat{B}^{i*} = 0, \qquad \hat{B}^{i*}_{,i} = 0,$$
$$\mathrm{i}\omega'\hat{j}^{0*}_\Omega + \hat{j}^{k*}_{\Omega,k} = 0, \qquad \mathrm{i}\omega'\hat{C}^{0*} + \hat{C}^{l*}_{,l} = 0. \tag{3.1}$$

Thus the fields in (2.4) and (2.5) refer to ω, e.g. $\hat{H}_j(\omega)$, $\varepsilon(\omega)$, $m_t^2(\omega)$, whereas the conjugated fields satisfying (3.1) are taken at ω', e.g. $\hat{H}^*_j(\omega')$, $\varepsilon^*(\omega')$, $m_t^{2*}(\omega')$, unless indicated otherwise.

We multiply the first inhomogeneous equation in (3.1) with $\hat{E}_k$ to find

$$\hat{j}^{k*}_\Omega\hat{E}_k = -\varepsilon^{jkl}\hat{H}^*_j\hat{E}_{k,l} - \left(\varepsilon^{lkj}\hat{H}^*_j\hat{E}_k\right)_{,l} - \mathrm{i}\omega'\hat{D}^{k*}\hat{E}_k - m_t^{2*}\hat{C}^{k*}\hat{E}_k. \tag{3.2}$$

We then multiply the first homogeneous equation in (2.7) with $\hat{H}^*_i$, $\varepsilon^{ink}\hat{H}^*_i\hat{E}_{n,k} + \mathrm{i}\omega\hat{H}^*_i\hat{B}^i = 0$, which we substitute for the first term. We also substitute $\hat{E}_k = \mathrm{i}\omega\hat{A}_k + \hat{A}_{0,k}$ into the $\hat{C}^{k*}\hat{E}_k$ term and use $\mathrm{i}\omega'\hat{C}^{0*} + \hat{C}^{l*}_{,l} = 0$. In this way, we can write (3.2) as

$$\hat{j}^{k*}_\Omega\hat{E}_k = \mathrm{i}\omega\hat{H}^*_i\hat{B}^i - \left(\varepsilon^{lkj}\hat{H}^*_j\hat{E}_k\right)_{,l} - \mathrm{i}\omega'\hat{D}^{k*}\hat{E}_k - m_t^{2*}\left(\mathrm{i}\omega\hat{C}^{k*}\hat{A}_k + \mathrm{i}\omega'\hat{C}^{0*}\hat{A}_0 + \left(\hat{C}^{k*}\hat{A}_0\right)_{,k}\right). \tag{3.3}$$

Here, we substitute the conjugated constitutive relations, cf. before (2.4),

$$\hat{j}^{k*}_\Omega\hat{E}_k = \left(\frac{\varepsilon^{ljk}\hat{B}^{j*}\hat{E}_k}{\mu^*(\omega')} - m_t^{2*}(\omega')\frac{\hat{A}^*_l\hat{A}_0}{\mu_0^*(\omega')}\right)_{,l} + \mathrm{i}\omega\left(\frac{\hat{B}^{i*}\hat{B}^i}{\mu^*(\omega')} - m_t^{2*}(\omega')\frac{\hat{A}^*_k\hat{A}_k}{\mu_0^*(\omega')}\right) - \mathrm{i}\omega'\left(\varepsilon^*(\omega')\hat{E}^*_k\hat{E}_k - m_t^{2*}(\omega')\varepsilon_0^*(\omega')\hat{A}^*_0\hat{A}_0\right). \tag{3.4}$$

We conjugate this equation and interchange $\omega \leftrightarrow \omega'$, so that the conjugated fields are again taken at ω'. Finally we consider $\hat{j}^{k*}_\Omega\hat{E}_k + \hat{j}^k_\Omega\hat{E}^*_k$, and expand the permeabilities at $\omega' = \omega$ in linear order,

$$\omega\varepsilon(\omega) - \omega'\varepsilon^*(\omega') = \left(\omega\varepsilon(\omega) - \omega\varepsilon^*(\omega)\right) - D_\varepsilon(\omega)(\omega' - \omega),$$
$$\frac{\omega}{\mu^*(\omega')} - \frac{\omega'}{\mu(\omega)} = \left(\frac{\omega}{\mu^*(\omega)} - \frac{\omega}{\mu(\omega)}\right) - D_\mu(\omega)(\omega' - \omega),$$
$$D_\varepsilon = \left(\omega\varepsilon^*(\omega)\right)', \qquad D_\mu = \frac{(\omega\mu^*(\omega))'}{\mu^{*2}(\omega)} + \frac{1}{\mu(\omega)} - \frac{1}{\mu^*(\omega)}. \tag{3.5}$$

Identical expansions hold for the rescaled permeabilities $\tilde{\varepsilon}_0 = m_t^2\varepsilon_0$ and $\tilde{\mu}_0 = \mu_0/m_t^2$. This rescaling just means to absorb the tachyonic mass-square in the Lagrangian into the permeability tensor $g_A^{\mu\nu}$, cf. (2.1) and (2.2). Thus we find, up to terms of $O((\omega' - \omega)^2)$,

$$\hat{S}^l_{,l} + \mathrm{i}(\omega' - \omega)\hat{\rho} = -\frac{1}{2}\left(\hat{j}^{k*}_\Omega\hat{E}_k + \hat{j}^k_\Omega\hat{E}^*_k\right) - \mathrm{i}\hat{j}, \tag{3.6}$$

where the flux vector $\hat{S}^l = \hat{T}^l_0$ reads

$$\hat{S}^l(\omega,\omega') = \frac{1}{2}\left(\frac{\varepsilon^{lkj}\hat{B}^{j*}\hat{E}_k}{\mu^*(\omega')} + \frac{\varepsilon^{lkj}\hat{E}^*_k\hat{B}^j}{\mu(\omega)} + \frac{m_t^{2*}(\omega')}{\mu_0^*(\omega')}\hat{A}^*_l\hat{A}_0 + \frac{m_t^2(\omega)}{\mu_0(\omega)}\hat{A}^*_0\hat{A}_l\right). \tag{3.7}$$

The conjugated fields are taken at ω', cf. after (3.1). The density $\hat{\rho} = \hat{T}^0_0$ in (3.6) is identified as

$$\hat{\rho}(\omega,\omega') = \frac{1}{2}\Bigg[\left(\omega\varepsilon^*(\omega)\right)'\hat{E}^*_k\hat{E}_k + \left(\frac{(\omega\mu^*(\omega))'}{\mu^{*2}(\omega)} + \frac{1}{\mu(\omega)} - \frac{1}{\mu^*(\omega)}\right)\hat{B}^{i*}\hat{B}^i - \left(\omega\tilde{\varepsilon}_0^*(\omega)\right)'\hat{A}^*_0\hat{A}_0 - \left(\frac{(\omega\tilde{\mu}_0^*(\omega))'}{\tilde{\mu}_0^{*2}(\omega)} + \frac{1}{\tilde{\mu}_0(\omega)} - \frac{1}{\tilde{\mu}_0^*(\omega)}\right)\hat{A}^*_k\hat{A}_k\Bigg], \tag{3.8}$$

where $\tilde{\varepsilon}_0 = m_t^2\varepsilon_0$ and $\tilde{\mu}_0 = \mu_0/m_t^2$. The energy absorption in the aether is quantified by the source term

$$\hat{j}(\omega,\omega') = \frac{1}{2}\Bigg[\left(\omega\varepsilon^*(\omega) - \omega\varepsilon(\omega)\right)\hat{E}^*_k\hat{E}_k - \left(\frac{\omega}{\mu^*(\omega)} - \frac{\omega}{\mu(\omega)}\right)\hat{B}^{i*}\hat{B}^i - m_t^2\left(\omega\varepsilon_0^*(\omega) - \omega\varepsilon_0(\omega)\right)\hat{A}^*_0\hat{A}_0 + m_t^2\left(\frac{\omega}{\mu_0^*(\omega)} - \frac{\omega}{\mu_0(\omega)}\right)\hat{A}^*_k\hat{A}_k\Bigg], \tag{3.9}$$

which vanishes for real non-absorptive permeabilities. To obtain a continuity equation, we multiply (3.6) with $e^{\mathrm{i}(\omega'-\omega)t}$ and write the second term on the left-hand side as time derivative $(\hat{\rho}e^{\mathrm{i}(\omega'-\omega)t})_{,t}$.

In the case of constant (frequency-independent) real permeabilities and tachyon mass, the conservation law (3.6) can be stated in spacetime representation as $S^l_{,l} + \rho_{,t} = -j^k_\Omega E_k$, where [5]

$$S^l(\mathbf{x},t) = T^l_0 = \varepsilon^{lkj}H_jE_k + m_t^2C^lA_0,$$
$$\rho(\mathbf{x},t) = T^0_0 = \frac{1}{2}\left(D^kE_k + H_kB^k\right) - \frac{m_t^2}{2}\left(C^kA_k + C_0A_0\right). \tag{3.10}$$

We use Fourier transforms $A_\mu = (2\pi)^{-1}\int_{-\infty}^{\infty}\hat{A}_\mu(\mathbf{x},\omega)e^{-\mathrm{i}\omega t}d\omega$ to write the Poynting vector in (3.10) as

$$S^l(\mathbf{x},t) = \frac{1}{(2\pi)^2}\int_{-\infty}^{+\infty}\left[\varepsilon^{lkj}\frac{1}{\mu}\hat{B}^{j*}(\omega')\hat{E}_k(\omega) + \frac{m_t^2}{\mu_0}\hat{A}^*_l(\omega')\hat{A}_0(\omega)\right]e^{\mathrm{i}(\omega'-\omega)t}d\omega d\omega'. \tag{3.11}$$

Since $S^l(\mathbf{x},t)$ is real, we can conjugate the integrand and interchange the integration variables, $\omega \leftrightarrow \omega'$. By taking the average, we find

$$S^l(\mathbf{x},t) = \frac{1}{(2\pi)^2}\int_{-\infty}^{+\infty}\hat{S}^l(\omega,\omega')e^{\mathrm{i}(\omega'-\omega)t}d\omega d\omega', \tag{3.12}$$

with $\hat{S}^l(\omega,\omega')$ in (3.7) and real constant permeabilities. In contrast to frequency-dependent permeabilities, expansion (3.5) leading to (3.6) is void in this case, so that ω' need not be close to ω.

We perform a time average of the flux vector (3.12), $\langle S^l\rangle = (1/T)\int_{-T/2}^{+T/2}S^l(\mathbf{x},t)dt$, to obtain

$$\langle S^l\rangle = \frac{1}{2\pi T}\int_{-\infty}^{\infty}\hat{S}^l(\omega,\omega')\delta_{(1),T}(\omega-\omega')d\omega d\omega', \tag{3.13}$$

where the time integration has been replaced by the limit definition $\delta_{(1),T}(\omega) = (2\pi)^{-1}\int_{-T/2}^{+T/2}e^{\mathrm{i}\omega t}dt$ of the Dirac delta function,

$\delta_{(1),T\to\infty}(\omega)=\delta(\omega)$. The mollifield distribution $\delta_{(1),T}$ is real and symmetric, $\delta_{(1),T}(\omega)=\delta_{(1),T}(-\omega)$. In radiation problems, the flux vector $\hat{S}^l(\omega,\omega')$ depends on the averaging period T as well, as it contains a product of the mollified delta functions $\delta_{(1),T}$, cf. (6.11) and (7.3). The $1/T$ factor in (3.13) is then needed to make this product well-defined in the limit $T\to\infty$, by virtue of a second limit definition of the delta function, $\delta_{(2),T}(\omega)=(2\pi/T)\delta^2_{(1),T}(\omega)$, $\delta_{(2),T\to\infty}(\omega)=\delta(\omega)$.

Since $\delta_{(1),T\to\infty}(\omega-\omega')$ in (3.13) converges to the delta function, we can replace $\hat{S}^l(\omega,\omega')$ by $\hat{S}^l(\omega,\omega)$. Thus this calculation of the averaged flux $\langle S^l\rangle$ also applies to dissipative complex permeabilities, as we only need the limit $\hat{S}^l(\omega,\omega'\to\omega)$, cf. (3.7), to perform a time average (with $T\to\infty$) of the Poynting flux vector. Analogously, we find the time-averaged energy density $\langle\rho\rangle$ by replacing $\hat{S}^l(\omega,\omega')$ in (3.13) by the spectral kernel $\hat{\rho}(\omega,\omega')$ in (3.8). These time averages are real, since $\hat{\rho}^*(\omega,\omega')=\hat{\rho}(-\omega,-\omega')$ and analogously for $\hat{S}^l(\omega,\omega')$, also see Section 4.

4. Transversal and longitudinal flux and energy components

We split the vector potential and the current into a transversal and longitudinal component, $\hat{\mathbf{A}}(\mathbf{x},\omega)=\hat{\mathbf{A}}^{\rm T}+\hat{\mathbf{A}}^{\rm L}$ with $\operatorname{div}\hat{\mathbf{A}}^{\rm T}=0$, $\operatorname{rot}\hat{\mathbf{A}}^{\rm L}=0$, and analogously the dressed current $\hat{\mathbf{j}}_\Omega(\mathbf{x},\omega)=\hat{\mathbf{j}}^{\rm T}_\Omega+\hat{\mathbf{j}}^{\rm L}_\Omega$, cf. Section 2, writing $\hat{\mathbf{A}}$ for $\hat{A}_k$ etc. We use current conservation, $i\omega\hat{\rho}_\Omega-\operatorname{div}\hat{\mathbf{j}}_\Omega=0$, $\hat{j}^\mu_\Omega=(\hat{\rho}_\Omega,\hat{\mathbf{j}}_\Omega)$, cf. (2.5), to split the charge density accordingly, $\hat{\rho}^{\rm T}_\Omega=0$, $i\omega\hat{\rho}^{\rm L}_\Omega=\operatorname{div}\hat{\mathbf{j}}^{\rm L}_\Omega$. The Lorentz condition, $\operatorname{div}\hat{\mathbf{A}}+i\omega\varepsilon_0\mu_0\hat{A}_0=0$, is employed to separate the transversal and longitudinal components of the scalar potential, $\hat{A}^{\rm T}_0=0$ and $\hat{A}^{\rm L}_0=-\operatorname{div}\hat{\mathbf{A}}^{\rm L}/(i\omega\varepsilon_0\mu_0)$. The polarized field strengths are $\hat{\mathbf{E}}^{\rm T}=i\omega\hat{\mathbf{A}}^{\rm T}$, $\hat{\mathbf{E}}^{\rm L}=i\omega\hat{\mathbf{A}}^{\rm L}+\nabla\hat{A}^{\rm L}_0$ and $\hat{\mathbf{B}}^{\rm L}=0$, $\hat{\mathbf{B}}^{\rm T}=\operatorname{rot}\hat{\mathbf{A}}^{\rm T}$.

The flux vectors of the transversal and longitudinal field components read, cf. (3.7),

$$\hat{\mathbf{S}}^{\mathrm{T}(j)}(\mathbf{x},\omega)=\frac{1}{2}\left(\hat{\mathbf{E}}^{\mathrm{T}(j)}\times\hat{\mathbf{B}}^{\mathrm{T}(j)*}\frac{1}{\mu^*}+\text{c.c.}\right),\tag{4.1}$$

$$\hat{\mathbf{S}}^{\rm L}(\mathbf{x},\omega)=-\frac{1}{2}\left(\frac{m_{\rm t}^{2*}}{\mu_0^*}\hat{\mathbf{A}}^{\rm L*}\hat{A}^{\rm L}_0+\text{c.c.}\right),\tag{4.2}$$

and the corresponding energy densities (3.8) are

$$\begin{aligned}\hat{\rho}^{\mathrm{T}(j)}(\mathbf{x},\omega)=\frac{1}{2}\bigg[&(\omega\varepsilon^*)'\hat{\mathbf{E}}^{\mathrm{T}(j)*}\hat{\mathbf{E}}^{\mathrm{T}(j)}\\&+\left(\frac{(\omega\mu^*)'}{\mu^{*2}}+\frac{1}{\mu}-\frac{1}{\mu^*}\right)\hat{\mathbf{B}}^{\mathrm{T}(j)*}\hat{\mathbf{B}}^{\mathrm{T}(j)}\\&-\left(\frac{(\omega\tilde{\mu}_0^*)'}{\tilde{\mu}_0^{*2}}+\frac{1}{\tilde{\mu}_0}-\frac{1}{\tilde{\mu}_0^*}\right)\hat{\mathbf{A}}^{\mathrm{T}(j)*}\hat{\mathbf{A}}^{\mathrm{T}(j)}\bigg],\end{aligned}\tag{4.3}$$

$$\begin{aligned}\hat{\rho}^{\rm L}(\mathbf{x},\omega)=\frac{1}{2}\bigg[&(\omega\tilde{\varepsilon}_0^*)'\hat{A}_0^{\rm L*}\hat{A}_0^{\rm L}+\left(\frac{(\omega\tilde{\mu}_0^*)'}{\tilde{\mu}_0^{*2}}+\frac{1}{\tilde{\mu}_0}-\frac{1}{\tilde{\mu}_0^*}\right)\hat{\mathbf{A}}^{\rm L*}\hat{\mathbf{A}}^{\rm L}\\&-(\omega\varepsilon^*)'\hat{\mathbf{E}}^{\rm L*}\hat{\mathbf{E}}^{\rm L}\bigg],\end{aligned}\tag{4.4}$$

where $\tilde{\varepsilon}_0=m_{\rm t}^2\varepsilon_0$ and $\tilde{\mu}_0=\mu_0/m_{\rm t}^2$. The index j labels two transversal degrees of freedom, cf. (6.8), and we have performed the limit $\omega'\to\omega$ in (3.7) and (3.8). We have also changed the sign of the longitudinal flux vector and energy density, to obtain a positive time average $\langle\rho^{\rm L}\rangle$, cf. (3.13),

$$\left\langle\mathbf{S}^{\mathrm{T}(j),\mathrm{L}},\rho^{\mathrm{T}(j),\mathrm{L}}\right\rangle=\frac{1}{2\pi T}\int_{-\infty}^{\infty}\left(\hat{\mathbf{S}}^{\mathrm{T}(j),\mathrm{L}},\hat{\rho}^{\mathrm{T}(j),\mathrm{L}}\right)(\mathbf{x},\omega;T)\,d\omega.\tag{4.5}$$

In the spectral densities, we have indicated their dependence on the averaging period $T\to\infty$, cf. after (3.13). $\hat{\mathbf{S}}^{\mathrm{T}(j),\mathrm{L}}(\mathbf{x},\omega;T)$ is real and symmetric in ω, and $\hat{\rho}^{\mathrm{T}(j),\mathrm{L}*}(\mathbf{x},\omega;T)=\hat{\rho}^{\mathrm{T}(j),\mathrm{L}}(\mathbf{x},-\omega;T)$, so that we can replace $\hat{\rho}^{\mathrm{T}(j),\mathrm{L}}$ by $\operatorname{Re}\hat{\rho}^{\mathrm{T}(j),\mathrm{L}}$ in the integrand of (4.5). We can also replace the lower integration boundary by zero and multiply the integral by a factor of two. In this way, we identify the spectral flux densities as $\hat{\mathbf{S}}^{\mathrm{T}(j),\mathrm{L}}(\mathbf{x},\omega;T)/(\pi T)$ and the associated spectral energy densities as $\operatorname{Re}\hat{\rho}^{\mathrm{T}(j),\mathrm{L}}(\mathbf{x},\omega;T)/(\pi T)$, to be understood in the limit $T\to\infty$.

5. Dissipative wave equations for the tachyonic vector potential

5.1. Transversal and longitudinal dispersion relations

Substituting the potential representation of the field strengths into the inhomogeneous field equations (2.4), we find the wave equations

$$\left(\Delta+m_{\rm t}^2\frac{\varepsilon_0}{\varepsilon}\right)\hat{A}_0+i\omega\operatorname{div}\hat{\mathbf{A}}=\frac{1}{\varepsilon}\hat{\rho}_\Omega,\tag{5.1}$$

$$\begin{aligned}&\left(\Delta+\kappa_{\rm T}^2\right)\hat{\mathbf{A}}-i\omega\varepsilon\mu\nabla\hat{A}_0-\nabla\operatorname{div}\hat{\mathbf{A}}=-\mu\hat{\mathbf{j}}_\Omega,\\&\kappa_{\rm T}^2(\omega)=\varepsilon\mu\omega^2+m_{\rm t}^2\frac{\mu}{\mu_0},\end{aligned}\tag{5.2}$$

where $\kappa_{\rm T}^2(\omega)$ is the transversal dispersion relation. We make use of the Lorentz condition and current conservation, cf. Section 4, to decouple the fields and to find the longitudinal dispersion relation,

$$\left(\Delta+\kappa_{\rm L}^2\right)\hat{A}_0=\frac{1}{\varepsilon}\hat{\rho}_\Omega,\qquad\kappa_{\rm L}^2(\omega)=\varepsilon_0\mu_0\omega^2+m_{\rm t}^2\frac{\varepsilon_0}{\varepsilon},\tag{5.3}$$

$$\left(\Delta+\kappa_{\rm T}^2\right)\hat{\mathbf{A}}+\left(\frac{\varepsilon}{\varepsilon_0}\frac{\mu}{\mu_0}-1\right)\nabla\operatorname{div}\hat{\mathbf{A}}=-\mu\hat{\mathbf{j}}_\Omega.\tag{5.4}$$

The wave equations (5.3) and (5.4), subject to the Lorentz condition and current conservation, are the basic evolution equations; Eq. (5.4) and the Lorentz condition lead to the scalar equation (5.3).

Transversal wave solutions of (5.3) and (5.4) are defined by the condition $\operatorname{div}\hat{\mathbf{A}}^{\rm T}=0$. The scalar component $\hat{A}^{\rm T}_0=0$ follows from the Lorentz condition. A transversal solution can only exist if the current is transversal, $\operatorname{div}\hat{\mathbf{j}}_\Omega=\hat{\rho}_\Omega=0$, cf. Section 4. Longitudinal wave solutions are defined by $\operatorname{rot}\hat{\mathbf{A}}^{\rm L}=0$. Applying the rotor to the vector equation (5.4), we see that longitudinal solutions can only exist if the current is longitudinal, $\operatorname{rot}\hat{\mathbf{j}}_\Omega=0$. Condition $\operatorname{rot}\hat{\mathbf{A}}^{\rm L}=0$ implies $\nabla\operatorname{div}\hat{\mathbf{A}}^{\rm L}=\Delta\hat{\mathbf{A}}^{\rm L}$, so that Eq. (5.4) can be written as $(\Delta+\kappa_{\rm L}^2)\hat{\mathbf{A}}^{\rm L}=-(\varepsilon_0\mu_0/\varepsilon)\hat{\mathbf{j}}_\Omega$, and $\hat{A}^{\rm L}_0$ is obtained from the Lorentz condition, $i\omega\varepsilon_0\mu_0\hat{A}^{\rm L}_0=-\operatorname{div}\hat{\mathbf{A}}^{\rm L}$.

5.2. Complex wavenumbers

We consider the complex squared wavenumbers $\kappa^2_{\rm T,L}(\omega)$ in (5.2) and (5.3), where $\varepsilon=\varepsilon_{\rm Re}+i\varepsilon_{\rm Im}$, $m_{\rm t}=m_{\rm t,Re}+im_{\rm t,Im}$, etc., with positive real parts of the permeabilities and tachyon mass. We split $\kappa^2_{\rm T,L}(\omega)=a_{\rm T,L}+ib_{\rm T,L}$ and expand in the imaginary parts of the permeabilities and mass; $a_{\rm T,L}$ then contains even powers and $b_{\rm T,L}$ odd ones. The transversal and longitudinal dispersion relations $\kappa^2_{\rm T,L}$ are related by the interchange $\varepsilon\leftrightarrow\mu_0$, $\mu\leftrightarrow\varepsilon_0$. We introduce the rescaled tachyon mass $\hat{m}_{\rm t}$,

$$\hat{m}_{\rm t,Re,Im}=\frac{m_{\rm t,Re,Im}}{\sqrt{\mu_{0,\rm Re}\varepsilon_{\rm Re}}},\tag{5.5}$$

and find in lowest order $\kappa^2_{\rm T,L}=a_{\rm T,L}+ib_{\rm T,L}$, where

$$a_{\rm T}\sim\varepsilon_{\rm Re}\mu_{\rm Re}\left(\omega^2+\hat{m}^2_{\rm t,Re}\right),\qquad a_{\rm L}\sim\mu_{0,\rm Re}\varepsilon_{0,\rm Re}\left(\omega^2+\hat{m}^2_{\rm t,Re}\right),\tag{5.6}$$

up to terms quadratic in the imaginary parts of the permeabilities, and

$$b_T \sim \varepsilon_{Re}\mu_{Re}\left[\left(\frac{\varepsilon_{Im}}{\varepsilon_{Re}}+\frac{\mu_{Im}}{\mu_{Re}}\right)\omega^2+\hat{m}^2_{t,Re}\left(\frac{\mu_{Im}}{\mu_{Re}}-\frac{\mu_{0,Im}}{\mu_{0,Re}}\right)+2\hat{m}_{t,Re}\hat{m}_{t,Im}\right],$$

$$b_L \sim \mu_{0,Re}\varepsilon_{0,Re}\left[\left(\frac{\mu_{0,Im}}{\mu_{0,Re}}+\frac{\varepsilon_{0,Im}}{\varepsilon_{0,Re}}\right)\omega^2+\hat{m}^2_{t,Re}\left(\frac{\varepsilon_{0,Im}}{\varepsilon_{0,Re}}-\frac{\varepsilon_{Im}}{\varepsilon_{Re}}\right)+2\hat{m}_{t,Re}\hat{m}_{t,Im}\right], \tag{5.7}$$

linear in the imaginary parts. The principal root $\kappa_{T,L} = \kappa_{T,L,Re} + i\kappa_{T,L,Im}$ of the squared wavenumbers $\kappa^2_{T,L}$ is given by $\kappa_{T,L,Re} \sim \sqrt{a_{T,L}}$ and $\kappa_{T,L,Im} \sim b_{T,L}/(2\sqrt{a_{T,L}})$. $\kappa_{T,L,Im}$ is thus linear in the imaginary parts of the permeabilities in lowest order (up to cubic terms in an ascending series expansion). The wavenumbers are defined by $k_{T,L}(\omega) = \mathrm{sign}(\kappa_{T,L,Im})\kappa_{T,L}$, see Section 6.1, and $\kappa_{T,L}$ satisfies the reality condition $\kappa^*_{T,L}(\omega) = \kappa_{T,L}(-\omega)$ like the permeabilities.

6. Retarded spherical wave propagation in the spacetime aether

6.1. Reduction to scalar transversal and longitudinal Green functions

We consider the scalar Green function satisfying

$$\left(\Delta+\kappa^2(\omega)\right)\hat{G}(\mathbf{x},\omega) = -\lambda(\omega)\delta(\mathbf{x}), \tag{6.1}$$

with complex $\kappa^2(\omega)$ and $\lambda(\omega)$ subject to the reality condition $\kappa^*(\omega) = \kappa(-\omega)$. Residual integration in momentum space gives

$$\hat{G}(\mathbf{x},\omega) = \frac{\lambda}{(2\pi)^3}\int \frac{e^{i\mathbf{kx}}d\mathbf{k}}{\mathbf{k}^2-\kappa^2(\omega)} = \frac{\lambda}{4\pi r}e^{i\,\mathrm{sign}(\kappa_{Im})\kappa r}, \tag{6.2}$$

where $\kappa = \kappa_{Re} + i\kappa_{Im}$. The Green function is unambiguously determined if κ^2 in the wave equation is complex, irrespectively of the sign of the root κ, and $\hat{G}^*(\mathbf{x},\omega) = \hat{G}(\mathbf{x},-\omega)$. The real part of the exponent gives the damping factor $\exp(-|\kappa_{Im}|r)$. The convention for Fourier time transforms is $G(\mathbf{x},t) = (2\pi)^{-1}\int \hat{G}(\mathbf{x},\omega)e^{-i\omega t}d\omega$. Thus, to obtain outgoing waves, the signs of κ_{Re} and κ_{Im} must coincide for positive frequencies and differ for negative ones. If the signs of κ_{Re} and κ_{Im} differ for positive frequencies, one has to switch to the second set of field equations defined by the conjugated permeability tensors, see before (2.3) and Section 5.2, otherwise one obtains incoming spherical waves, that is an advanced Green's function in space-frequency representation. If both κ_{Re} and κ_{Im} are positive for positive frequencies, we can replace $\mathrm{sign}(\kappa_{Im})$ by $\mathrm{sign}(\omega)$ in (6.2).

The wave equations for transversal and longitudinal radiation fields read $(\Delta+\kappa^2_{T,L})\hat{\mathbf{A}}^{T,L} = -\lambda^{T,L}\hat{\mathbf{j}}^{T,L}_{\Omega}$, with $\lambda^T = \mu$ and $\lambda^L = \varepsilon_0\mu_0/\varepsilon$, cf. Section 5.1. The corresponding Green functions are defined by $(\Delta+\kappa^2_{T,L})\hat{G}^{T,L}(\mathbf{x},\omega) = -\lambda^{T,L}\delta(\mathbf{x})$, and wave solutions are found as

$$\hat{\mathbf{A}}^{T,L}(\mathbf{x},\omega) = \int \hat{G}^{T,L}\left(\mathbf{x}-\mathbf{x}',\omega\right)\hat{\mathbf{j}}^{T,L}_{\Omega}\left(\mathbf{x}',\omega\right)d\mathbf{x}',$$

$$\hat{G}^{T,L}(\mathbf{x},\omega) = \frac{\lambda^{T,L}}{4\pi|\mathbf{x}|}e^{ik_{T,L}|\mathbf{x}|}. \tag{6.3}$$

The wavenumbers are $k_{T,L} = \mathrm{sign}(\kappa_{T,L,Im})\kappa_{T,L}$, so that $k_{T,L}(-\omega) = -k^*_{T,L}(\omega)$, in contrast to the reality condition for permeabilities.

6.2. Asymptotic tachyon fields

In the Green function $\hat{G}^{T,L}(\mathbf{x}-\mathbf{x}',\omega)$ in (6.3), we put $\mathbf{n} = \mathbf{x}/r$ with $r = |\mathbf{x}|$ and $|\mathbf{x}'|/r \ll 1$, and expand $|\mathbf{x}-\mathbf{x}'| = r(1-\mathbf{nx}'/r+\cdots)$, to obtain the dipole approximation

$$\hat{G}^{T,L}\left(\mathbf{x}-\mathbf{x}',\omega\right) \sim \frac{\lambda^{T,L}}{4\pi r}e^{ik_{T,L}r}e^{-ik_{T,L,Re}\mathbf{nx}'},$$

$$\nabla_{\mathbf{x}}\hat{G}^{T,L} \sim \mathbf{n}ik_{T,L}\hat{G}^{T,L}. \tag{6.4}$$

By substituting this into the integral representation (6.3), we find the asymptotic wave fields

$$\hat{\mathbf{A}}^{T,L}(\mathbf{x},\omega) \sim \frac{1}{\Omega}\frac{\lambda^{T,L}}{4\pi r}e^{ik_{T,L}r}\int e^{-ik_{T,L,Re}\mathbf{nx}'}\hat{\mathbf{j}}^{T,L}\left(\mathbf{x}',\omega\right)d\mathbf{x}', \tag{6.5}$$

and note $\mathrm{div}\,\hat{\mathbf{A}}^L \sim ik_L\mathbf{n}\hat{\mathbf{A}}^L$, $\nabla\,\mathrm{div}\,\hat{\mathbf{A}}^L \sim -k_L^2\hat{\mathbf{A}}^L$ and $\mathrm{rot}\,\hat{\mathbf{A}}^T \sim ik_T\mathbf{n}\times\hat{\mathbf{A}}^T$. The transversal and longitudinal current components, cf. Section 4, are defined with regard to the radial unit wave vector $\mathbf{n}$, so that $\mathbf{n}\hat{\mathbf{j}}^T = 0$, and $\mathbf{n}\times\hat{\mathbf{j}}^L = 0$. We will use the current transform

$$\hat{\mathbf{j}}(k_{T,L,Re}) = \int d\mathbf{x}'\,\hat{\mathbf{j}}\left(\mathbf{x}',\omega\right)\exp\left(-ik_{T,L,Re}(\omega)\mathbf{nx}'\right), \tag{6.6}$$

projected onto a triad of orthonormal polarization vectors $\boldsymbol{\varepsilon}_{1,2}(\mathbf{n})$ and $\mathbf{n}$,

$$\hat{\mathbf{j}}^{T(j)}(\mathbf{x},\omega) = \boldsymbol{\varepsilon}_j\left(\boldsymbol{\varepsilon}_j\hat{\mathbf{j}}(k_{T,Re})\right), \qquad \hat{\mathbf{j}}^L(\mathbf{x},\omega) = \mathbf{n}\left(\mathbf{n}\hat{\mathbf{j}}(k_{L,Re})\right). \tag{6.7}$$

Here, $\mathbf{n} = \mathbf{x}/r$ is the unit wave vector of the spherical wave identified as longitudinal polarization vector, and $\boldsymbol{\varepsilon}_{1,2}$ are transversal polarization vectors defining two degrees of linear polarization. To settle the angular parametrization of the polarization vectors, we use the Cartesian coordinate unit vector $\mathbf{e}_3$ as polar axis, $\mathbf{ne}_3 = \cos\theta$. (In Section 7, $\mathbf{e}_3$ will be identified with the unit velocity vector $\boldsymbol{\upsilon}_0$ of the radiating inertial charge.) As for the polarization triad, we use two real transversal polarization vectors $\boldsymbol{\varepsilon}_{1,2}$, so that $\boldsymbol{\varepsilon}_1$, $\boldsymbol{\varepsilon}_2$ and $\mathbf{n}$ constitute a right-handed triad. We choose $\boldsymbol{\varepsilon}_1$ orthogonal to $\mathbf{n}$ and $\mathbf{e}_3$, and place $\boldsymbol{\varepsilon}_2$ into the plane generated by $\mathbf{n}$ and $\mathbf{e}_3$,

$$\boldsymbol{\varepsilon}_1 = \frac{\mathbf{e}_3\times\mathbf{n}}{\sqrt{1-(\mathbf{ne}_3)^2}}, \qquad \boldsymbol{\varepsilon}_2 = \frac{\mathbf{e}_3-\mathbf{n}(\mathbf{ne}_3)}{\sqrt{1-(\mathbf{ne}_3)^2}}, \tag{6.8}$$

so that $\mathbf{n} = \boldsymbol{\varepsilon}_1\times\boldsymbol{\varepsilon}_2$, cyclically, and $\boldsymbol{\varepsilon}_1\mathbf{e}_3 = 0$, $\boldsymbol{\varepsilon}_2\mathbf{e}_3 = \sin\theta$. Accordingly, cf. (6.5),

$$\hat{\mathbf{A}}^{T(j),L}(\mathbf{x},\omega) \sim \frac{1}{\Omega}\frac{\lambda^{T,L}}{4\pi r}e^{ik_{T,L}r}\hat{\mathbf{j}}^{T(j),L}(\mathbf{x},\omega), \tag{6.9}$$

with $\lambda^T = \mu$, $\lambda^L = \varepsilon_0\mu_0/\varepsilon$ and $\mathbf{n}\times\hat{\mathbf{j}}^{T(1)} = \boldsymbol{\varepsilon}_2(\boldsymbol{\varepsilon}_1\hat{\mathbf{j}}(k_{T,Re}))$, $\mathbf{n}\times\hat{\mathbf{j}}^{T(2)} = -\boldsymbol{\varepsilon}_1(\boldsymbol{\varepsilon}_2\hat{\mathbf{j}}(k_{T,Re}))$.

As pointed out in Sections 4 and 5.1, the transversal fields are $\hat{A}_0^{T(j)} = 0$, $\hat{\mathbf{E}}^{T(j)} = i\omega\hat{\mathbf{A}}^{T(j)}$, $\hat{\mathbf{B}}^{T(j)} = \mathrm{rot}\,\hat{\mathbf{A}}^{T(j)}$, and the longitudinal ones read $\hat{A}_0^L = -\mathrm{div}\,\hat{\mathbf{A}}^L/(i\omega\varepsilon_0\mu_0)$, $\hat{\mathbf{B}}^L = 0$, and $\hat{\mathbf{E}}^L = i\omega\hat{\mathbf{A}}^L + \nabla\hat{A}_0^L$ with $\nabla\hat{A}_0^L = -\Delta\hat{\mathbf{A}}^L/(i\omega\varepsilon_0\mu_0)$, so that, by way of the dispersion relation in (5.3),

$$\nabla\hat{A}_0^L \sim \frac{k_L^2}{i\omega\varepsilon_0\mu_0}\hat{\mathbf{A}}^L, \qquad \hat{\mathbf{E}}^L \sim \frac{m_t^2}{i\omega\mu_0\varepsilon}\hat{\mathbf{A}}^L. \tag{6.10}$$

The asymptotic energy flux is found by substituting these fields into Eqs. (4.1) and (4.2),

$$\hat{\mathbf{S}}^{T(j)}(\mathbf{x},\omega) \sim \frac{e^{-2k_{T,Im}r}}{(4\pi r)^2}\frac{\mathrm{Re}(\mu k_T^*)\omega}{\Omega\Omega^*}\mathbf{n}\left(\hat{\mathbf{j}}^{T(j)}(\mathbf{x},\omega)\hat{\mathbf{j}}^{T(j)*}(\mathbf{x},\omega)\right),$$

$$\hat{\mathbf{S}}^L(\mathbf{x},\omega) \sim \frac{e^{-2k_{L,Im}r}}{(4\pi r)^2}\frac{\mathrm{Re}(m_t^{2*}\varepsilon_0^*k_L)}{\omega\varepsilon\varepsilon^*\Omega\Omega^*}\mathbf{n}\left(\hat{\mathbf{j}}^L(\mathbf{x},\omega)\hat{\mathbf{j}}^{L*}(\mathbf{x},\omega)\right), \tag{6.11}$$

valid at large distance r from the source. The spectral energy densities $\hat{\rho}^{T(j),L}(\mathbf{x},\omega)$ in (4.3) and (4.4) can be expressed analogously. The time-averaged flux vectors are obtained as $\langle\hat{\mathbf{S}}^{T(j),L}\rangle = \int_0^\infty\hat{\mathbf{S}}^{T(j),L}(\mathbf{x},\omega;T)d\omega/(\pi T)$ in the limit $T\to\infty$, see after (3.13), (4.5) and (7.1).

7. Dissipative tachyonic Cherenkov densities

We consider a subluminal particle $\mathbf{x}_0(t)$ moving in the vicinity of the coordinate origin and carrying a tachyonic charge q. The charge and current densities are $j^0 = \rho = q\delta(\mathbf{x} - \mathbf{x}_0(t))$ and $\mathbf{j}(\mathbf{x}, t) = q\dot{\mathbf{x}}_0\delta(\mathbf{x} - \mathbf{x}_0(t))$, so that the current transform (6.6) reads

$$\hat{\mathbf{j}}(k_{\mathrm{T,L,Re}}; T) = q \int_{-T/2}^{+T/2} \exp\left[-\mathrm{i}\left(k_{\mathrm{T,L,Re}}\mathbf{n}\mathbf{x}_0(t) - \omega t\right)\right]\mathrm{d}\mathbf{x}_0(t). \tag{7.1}$$

The time cutoff $T \to \infty$ has been introduced as a regularization to make squares of delta functions appearing in the flux vectors well-defined. In this way, the current transform depends on the averaging period T in (4.5), and so do the flux vectors $\hat{\mathbf{S}}^{\mathrm{T}(j)}(\mathbf{x}, \omega; T)$ in (6.11).

We specialize to uniform motion $\mathbf{x}_0(t) = \boldsymbol{\upsilon} t$, where $\boldsymbol{\upsilon}$ is the subluminal speed $\upsilon < 1$, and use $\boldsymbol{\upsilon}$ as polar axis, $\boldsymbol{\upsilon} = \upsilon\mathbf{e}_3$, $\mathbf{n}\boldsymbol{\upsilon} = \upsilon\cos\theta$, cf. (6.8), to obtain

$$\hat{\mathbf{j}}(k_{\mathrm{T,L,Re}}; T) = q\upsilon\mathbf{e}_3 \int_{-T/2}^{+T/2} \exp\left[-\mathrm{i}(k_{\mathrm{T,L,Re}}\upsilon\cos\theta - \omega)t\right]\mathrm{d}t. \tag{7.2}$$

The time integral is a limit definition $\delta_{(1),T}(\omega)$ of the Dirac function stated after (3.13). The polarization components (6.7) then read

$$\hat{\mathbf{j}}^{\mathrm{T}(j)}(\mathbf{x}, \omega; T) = 2\pi q\upsilon\delta_{(1),T}(k_{\mathrm{T,Re}}\upsilon\cos\theta - \omega)\boldsymbol{\varepsilon}_j(\boldsymbol{\varepsilon}_j\mathbf{e}_3),$$
$$\hat{\mathbf{j}}^{\mathrm{L}}(\mathbf{x}, \omega; T) = 2\pi q\upsilon\delta_{(1),T}(k_{\mathrm{L,Re}}\upsilon\cos\theta - \omega)\mathbf{n}(\mathbf{n}\mathbf{e}_3). \tag{7.3}$$

Thus $\hat{\mathbf{j}}^{\mathrm{T}(1)} = 0$, since $\boldsymbol{\varepsilon}_1\mathbf{e}_3 = 0$, $\boldsymbol{\varepsilon}_2\mathbf{e}_3 = \sin\theta$, $\mathbf{n}\mathbf{e}_3 = \cos\theta$, cf. after (6.8), so that the transversal radiation is linearly polarized in the $\boldsymbol{\varepsilon}_2$ direction. By substituting (7.3) into the flux vectors (6.11) and replacing $\delta^2_{(1),T} \to T\delta_{(2),T}/(2\pi)$, cf. after (3.13), we find the time averages (defined after (6.11)):

$$\left\langle \mathbf{S}^{\mathrm{T}(i)} \right\rangle \sim 2\frac{q^2\upsilon^2\mathbf{n}}{(4\pi r)^2}(\boldsymbol{\varepsilon}_i\mathbf{e}_3)^2 \times \int_0^\infty \mathrm{e}^{-2k_{\mathrm{T,Im}}r}\frac{\mathrm{Re}(\mu k_{\mathrm{T}}^*)\omega}{\Omega\Omega^*}\delta_{(2),T}(k_{\mathrm{T,Re}}\upsilon\cos\theta - \omega)\mathrm{d}\omega,$$
$$\left\langle \mathbf{S}^{\mathrm{L}} \right\rangle \sim 2\frac{q^2\upsilon^2\mathbf{n}}{(4\pi r)^2}(\mathbf{n}\mathbf{e}_3)^2 \times \int_0^\infty \mathrm{e}^{-2k_{\mathrm{L,Im}}r}\frac{\mathrm{Re}(m_{\mathrm{t}}^{2*}\varepsilon_0^* k_{\mathrm{L}})}{\omega\varepsilon\varepsilon^*\Omega\Omega^*}\delta_{(2),T}(k_{\mathrm{L,Re}}\upsilon\cos\theta - \omega)\mathrm{d}\omega. \tag{7.4}$$

Performing the limit $T \to \infty$, we can replace $\delta_{(2),T}$ by the delta function, $\delta_{(2),T} \to \delta$. The Cherenkov emission angle between particle velocity $\boldsymbol{\upsilon}$ and radial wave vector $k_{\mathrm{T,L,Re}}\mathbf{n}$ is thus $\cos\theta_{\mathrm{T,L}} = \omega/(k_{\mathrm{T,L,Re}}\upsilon)$. The transversal flux is $\langle\mathbf{S}^{\mathrm{T}}\rangle = \langle\mathbf{S}^{\mathrm{T}(2)}\rangle$ since $\langle\mathbf{S}^{\mathrm{T}(1)}\rangle = 0$ (in the classical limit). The radiant power is obtained by integrating the normal projection of the flux through a sphere of large radius r, $P^{\mathrm{T,L}} \sim r^2\int\langle\mathbf{S}^{\mathrm{T,L}}\rangle\mathbf{n}\mathrm{d}\Omega$, where $\mathrm{d}\Omega$ is the solid-angle element. Thus, $P^{\mathrm{T,L}} \sim 2\pi r^2\int_{-1}^{1}\langle\mathbf{S}^{\mathrm{T,L}}\rangle\mathbf{n}\mathrm{d}y$, with $\cos\theta = y$ in the flux vectors (7.4). We extend the integration boundaries to infinity by substituting the Heaviside step function $\Theta(1 - |y|)$ into the integrand and perform the $\mathrm{d}y$ integration:

$$P^{\mathrm{T}} \sim \frac{q^2\upsilon}{4\pi}\int_0^\infty \mathrm{e}^{-2k_{\mathrm{T,Im}}r}\frac{\omega}{k_{\mathrm{T,Re}}}\frac{\mathrm{Re}(\mu k_{\mathrm{T}}^*)}{\Omega\Omega^*}\left(1 - \frac{\omega^2}{k_{\mathrm{T,Re}}^2\upsilon^2}\right) \times \Theta\left(1 - \frac{\omega}{k_{\mathrm{T,Re}}\upsilon}\right)\mathrm{d}\omega,$$
$$P^{\mathrm{L}} \sim \frac{q^2}{4\pi\upsilon}\int_0^\infty \mathrm{e}^{-2k_{\mathrm{L,Im}}r}\frac{\omega}{k_{\mathrm{L,Re}}^3}\frac{\mathrm{Re}(m_{\mathrm{t}}^{2*}\varepsilon_0^* k_{\mathrm{L}})}{\Omega\Omega^*\varepsilon\varepsilon^*}\Theta\left(1 - \frac{\omega}{k_{\mathrm{L,Re}}\upsilon}\right)\mathrm{d}\omega. \tag{7.5}$$

In the exponential, we expand $k_{\mathrm{T,L,Im}}$ in the imaginary parts of the permeabilities, retaining only the leading order, which is linear in the imaginary parts, cf. after (5.7). The attenuation length $1/(2k_{\mathrm{T,L,Im}})$ differs for transversal and longitudinal modes. All other terms in the integrands only depend quadratically on the imaginary parts of the permeabilities, which we neglect, $\mathrm{Re}(\mu k_{\mathrm{T}}^*) \sim \mu_{\mathrm{Re}}k_{\mathrm{T,Re}}$, $\mathrm{Re}(m_{\mathrm{t}}^{2*}\varepsilon_0^* k_{\mathrm{L}}) \sim m_{\mathrm{t,Re}}^2\varepsilon_{0,\mathrm{Re}}k_{\mathrm{L,Re}}$. For instance, in the photonic case, we put $m_{\mathrm{t}} = 0$, $\Omega = 1$, and substitute $k_{\mathrm{T,Re}} \sim \sqrt{\varepsilon_{\mathrm{Re}}\mu_{\mathrm{Re}}}\omega$ and $2k_{\mathrm{T,Im}} \sim (\varepsilon_{\mathrm{Im}}\mu_{\mathrm{Re}} + \mu_{\mathrm{Im}}\varepsilon_{\mathrm{Re}})\omega/\sqrt{\varepsilon_{\mathrm{Re}}\mu_{\mathrm{Re}}}$ into P^{T}, cf. Section 5.2; the power longitudinally radiated vanishes. The permeabilities differ for tachyons and photons, as well as the respective fine-structure constants, cf. after (7.8) and Ref. [19]. By means of (7.5), we identify the spectral densities determining the power $P^{\mathrm{T,L}} = \int_0^\infty p^{\mathrm{T,L}}(\omega, \gamma)\mathrm{d}\omega$ measured at large distance d from the source particle as

$$p^{\mathrm{T}}(\omega, \gamma) = \frac{q^2}{4\pi}\mathrm{e}^{-2k_{\mathrm{T,Im}}d}\frac{\mu_{\mathrm{Re}}}{\Omega_{\mathrm{Re}}^2}\frac{M_{\mathrm{T}}^2\omega}{\omega^2 + M_{\mathrm{T}}^2}\left(\gamma^2 - 1 - \frac{\omega^2}{M_{\mathrm{T}}^2}\right)\frac{\Theta(D_{\mathrm{t}}^{\mathrm{T}})}{\gamma\sqrt{\gamma^2 - 1}},$$
$$p^{\mathrm{L}}(\omega, \gamma) = \frac{q^2}{4\pi}\mathrm{e}^{-2k_{\mathrm{L,Im}}d}\frac{\varepsilon_{0,\mathrm{Re}}\mu_{0,\mathrm{Re}}}{\Omega_{\mathrm{Re}}^2\varepsilon_{\mathrm{Re}}}\frac{\hat{m}_{\mathrm{t,Re}}^2\omega}{\omega^2 + M_{\mathrm{L}}^2}\frac{\gamma\Theta(D_{\mathrm{t}}^{\mathrm{L}})}{\sqrt{\gamma^2 - 1}}. \tag{7.6}$$

Here, we parametrized the particle velocity with the Lorentz factor, $\upsilon = \sqrt{\gamma^2 - 1}/\gamma$, and introduced the generalized real mass-squares

$$M_{\mathrm{T}}^2 = (\varepsilon_{\mathrm{Re}}\mu_{\mathrm{Re}} - 1)\omega^2 + \hat{m}_{\mathrm{t,Re}}^2\varepsilon_{\mathrm{Re}}\mu_{\mathrm{Re}},$$
$$M_{\mathrm{L}}^2 = (\varepsilon_{0,\mathrm{Re}}\mu_{0,\mathrm{Re}} - 1)\omega^2 + \hat{m}_{\mathrm{t,Re}}^2\varepsilon_{0,\mathrm{Re}}\mu_{0,\mathrm{Re}}, \tag{7.7}$$

where $\hat{m}_{\mathrm{t,Re}} = m_{\mathrm{t,Re}}/\sqrt{\mu_{0,\mathrm{Re}}\varepsilon_{\mathrm{Re}}}$, cf. (5.5), so that the real part of the wavenumber is $k_{\mathrm{T,L,Re}} \sim \sqrt{\omega^2 + M_{\mathrm{T,L}}^2}$ in leading order, cf. (5.6). The argument in the step function in (7.6) reads

$$D_{\mathrm{t}}^{\mathrm{T,L}}(\omega, \gamma) = \sqrt{\omega^2 + M_{\mathrm{T,L}}^2}\frac{\sqrt{\gamma^2 - 1}}{\gamma} - \omega. \tag{7.8}$$

The constant $q^2/(4\pi\hbar c) = \alpha_{\mathrm{t0}}$ in (7.6) is the tachyonic counterpart to the electric fine-structure constant $e^2/(4\pi\hbar c) = 1/137$, and $\Omega\Omega^* \sim \Omega_{\mathrm{Re}}^2(\omega)$ is the scale factor of the frequency-dependent tachyonic fine-structure constant $\alpha_{\mathrm{t}}(\omega) = \alpha_{\mathrm{t0}}/\Omega_{\mathrm{Re}}^2(\omega)$, cf. after (2.2) and Ref. [9]. $D_{\mathrm{t}}^{\mathrm{T,L}}(\omega, \gamma)$ can only be positive if the mass-square $M_{\mathrm{T,L}}^2$ is positive, which is thus a radiation condition. Moreover, condition $M_{\mathrm{T,L}}^2/m^2 \ll 1$ has to be satisfied, where m is the mass of the radiating charge, otherwise the classical radiation densities have to be replaced by the quantized ones; the latter depend on the particle mass m and converge to the classical densities in the limit $m \to \infty$, see Ref. [26] for tachyonic quantum densities (with non-absorptive real permeabilities) and their limit cases. We solve $D_{\mathrm{t}}^{\mathrm{T,L}}(\omega, \gamma) = 0$ for γ to find the minimal Lorentz factor $\gamma_{\mathrm{T,L}}(\omega) = \sqrt{1 + \omega^2/M_{\mathrm{T,L}}^2}$ for Cherenkov emission; a frequency ω can only be radiated by a charge whose Lorentz factor exceeds $\gamma_{\mathrm{T,L}}(\omega)$.

8. Cherenkov spectral fit to supernova remnant RX J1713.7 – 3946

We average the tachyonic Cherenkov densities (7.6) over a relativistic thermal electron distribution, $\mathrm{d}\rho(\gamma) = A_\beta \mathrm{e}^{-\beta\gamma}\sqrt{\gamma^2 - 1} \times \gamma\mathrm{d}\gamma$, parametrized with the electronic Lorentz factor γ. A_β is the normalization constant, $\beta = m/(k_B T)$ the temperature parameter and m the electron mass. The differential energy flux $F_\omega^{T,L}$ and number flux $dN^{T,L}/d\omega$ read

$$F_\omega^{T,L} = \omega \frac{dN^{T,L}}{d\omega} = \frac{\langle p^{T,L}\rangle}{4\pi d^2},$$
$$\langle p^{T,L}\rangle = \int_{\gamma_{T,L}(\omega)}^{\infty} p^{T,L}(\omega,\gamma)\, d\rho(\gamma), \tag{8.1}$$

where $\langle p^{T,L}\rangle$ are the averaged transversal/longitudinal Cherenkov densities (7.6), d is the distance to the source, and $\gamma_{T,L}(\omega) = \sqrt{1+\omega^2/M_{T,L}^2}$ the minimal Lorentz factor, cf. after (7.8). The total energy flux is thus $\omega F_\omega^{T+L}[\mathrm{GeV\,cm^{-2}\,s^{-1}}] = \omega(F_\omega^T + F_\omega^L)$ with polarization components

$$\omega F_\omega^T = \frac{a_t \mu_{Re}(\omega)}{\Omega_{Re}^2(\omega)} e^{-2k_{T,Im}(\omega)d} \omega \frac{e^{-\beta\gamma_T(\omega)}}{\gamma_T^2(\omega)} \bigl(2 + 2\beta\gamma_T(\omega)\bigr),$$
$$\omega F_\omega^L = \frac{a_t \mu_{Re}}{\Omega_{Re}^2} \frac{\varepsilon_{0,Re}\mu_{0,Re}}{\varepsilon_{Re}\mu_{Re}} \frac{\hat{m}_{t,Re}^2}{M_L^2} e^{-2k_{L,Im}d} \omega \frac{e^{-\beta\gamma_L}}{\gamma_L^2(\omega)} \times \bigl(2 + 2\beta\gamma_L + \beta^2\gamma_L^2\bigr). \tag{8.2}$$

The flux amplitude is $a_t = \alpha_{t0} A_\beta/(4\pi d^2 \beta^3)$ with $\alpha_{t0} = q^2/(4\pi)$.

We specify the permeabilities as $\varepsilon_{Re}\mu_{Re} = \varepsilon_{0,Re}\mu_{0,Re} = 1$, and put their imaginary parts to zero, so that the permeability tensors (2.2) are conformal to the Minkowski metric. The transversal/longitudinal dispersion relations in (5.2) and (5.3) are then identical, and we drop the subscripts T and L of the wavenumbers $k = k_{Re} + ik_{Im}$, which are complex because of the imaginary part of the tachyon mass, cf. Section 5.2. The minimal Lorentz factor $\gamma_{T,L}(\omega)$ in the flux densities (8.2) can be replaced by $\gamma_{min}(\omega) = \sqrt{1+\omega^2/\hat{m}_{t,Re}^2}$, since $M_{T,L}^2 = \hat{m}_{t,Re}^2$, cf. (7.7). We rescale the tachyonic fine-structure constant $\alpha_t = \alpha_{t0}/\Omega_{Re}^2$, cf. after (7.8), with the magnetic permeability, $\hat{\alpha}_t = \alpha_t \mu_{Re}$, and specify the frequency dependence of $\hat{\alpha}_t$ and the rescaled tachyon mass $\hat{m}_{t,Re}$ in (7.7) as power laws: $\hat{\alpha}_t(\omega) = \hat{\alpha}_{t0}\omega^\sigma$ and $\hat{m}_{t,Re}(\omega) = \hat{m}_{t0}\omega^\rho$. In the flux densities (8.2), we substitute

$$\frac{a_t \mu_{Re}(\omega)}{\Omega_{Re}^2(\omega)} = \frac{A_F}{\hat{m}_{t0}^2}\omega^\sigma, \qquad A_F := \frac{A_\beta \hat{\alpha}_{t0}\hat{m}_{t0}^2}{4\pi d^2 \beta^3}. \tag{8.3}$$

Finally, we consider a frequency interval where the energy of the radiated quanta is much larger than the tachyon mass, $\hat{m}_{t,Re}^2/\omega^2 \ll 1$ (to be satisfied in addition to $\hat{m}_{t,Re}^2/m^2 \ll 1$, where m is the electron mass, see after (7.8)), and approximate the minimal Lorentz factor by $\gamma_{min}(\omega) \sim \omega/\hat{m}_{t,Re}$, so that $\beta\gamma_{min} \sim \hat{\beta}\omega^{1-\rho}$, with $\hat{\beta} = \beta/\hat{m}_{t0}$. The unpolarized flux (8.2) thus reads

$$\omega F_\omega^{T+L} \sim A_F e^{-2k_{Im}(\omega)d} \omega^\eta e^{-\hat{\beta}\omega^{1-\rho}} \bigl(4 + 4\hat{\beta}\omega^{1-\rho} + \bigl(\hat{\beta}\omega^{1-\rho}\bigr)^2\bigr), \tag{8.4}$$

with exponent $\eta = \sigma + 2\rho$, cf. before (8.3). This approximation holds uniformly in a finite frequency interval (defined by the data sets) if the tachyonic mass amplitude $\hat{m}_{t0}$ is sufficiently small. The spectral fit to SNR RX J1713.7 − 3946 in Fig. 1 is performed with flux density (8.4). Since $\hat{m}_{t0}$ is small and $\hat{\beta}$ is moderate, cf. the caption to Fig. 1, the electronic temperature parameter β is small as well, cf. before (8.1), so that the radiating electron plasma is ultra-relativistic.

The imaginary part of the wavenumber in the first exponential of flux density (8.4) is $k_{Im} \sim \hat{m}_{t,Re}\hat{m}_{t,Im}/\omega$, cf. after (5.7) and (6.3). The scaling relation $\hat{m}_{t,Im}(\omega) = \hat{m}_{t1}\omega^\chi$ for the imaginary part of the tachyon mass (analogous to the frequency scaling of the real part, see before (8.3)) gives $k_{Im}(\omega) \sim \hat{m}_{t0}\hat{m}_{t1}\omega^{\rho+\chi-1}$. In the spectral fit, we assume the tachyonic attenuation length $1/(2k_{Im})$ in the considered frequency interval to be much larger than the source distance $d \approx 1\mathrm{kpc}$ and put $\exp(-2k_{Im}d) \approx 1$. The second attenuation factor $\exp(-\hat{\beta}\omega^{1-\rho})$ in (8.4) causes the subexponential Weibull decay [9,26] of the spectral tail depicted in Fig. 1. The tachyonic group velocity $\upsilon_{gr} = 1/k'_{Re}$ (with $k_{Re} \sim \sqrt{\omega^2 + \hat{m}_{t,Re}^2}$, cf. (5.6) and Ref. [27]) reads $\upsilon_{gr}(\omega) - 1 \sim (1/2 - \rho)\omega^{2\rho-2}\hat{m}_{t0}^2$, valid in the limit $\hat{m}_{t,Re}^2/\omega^2 \ll 1$, which is the approximation used in flux density (8.4). In the case of SNR RX J1713.7 − 3946, the velocity of the tachyonic γ-rays is subluminal due to the scaling exponent $\rho \approx 0.75$ of the tachyon mass, see the caption to Fig. 1.

9. Conclusion

We have developed a practically viable formalism to treat tachyonic Maxwell–Proca radiation fields in the absorptive spacetime aether [28–31], in particular, to identify the spectral flux and the associated energy density. In Section 3, we discussed the dissipating energy flux, and the stress tensor can be dealt with analogously; to derive the conservation law for the field momentum, one starts with the Lorentz force, $\hat{j}_\Omega^{0*}\hat{E}_m + \varepsilon_{mij}\hat{j}_\Omega^{i*}\hat{B}^j$, instead of $\hat{j}_\Omega^{k*}\hat{E}_k$ in (3.2). Because of dispersion and energy dissipation manifested by the absorption term in the energy conservation law, the time averaging explained in Section 3 is necessary to extract the spectral energy and flux densities intrinsic to the radiation field. The spacetime aether is defined by homogeneous and isotropic permeability tensors, cf. Section 2. Therefore, it is crucial to unambiguously identify the intrinsic field energy subject to persistent dissipation, since it is not possible to deal with energy by striking the balance between asymptotic fields (in- and out-states) in non-dissipative vacuum regions, as the latter do not exist.

The complex Lagrangian (2.1) in space-frequency representation allows for a manifestly covariant formulation of the field equations and the constitutive relations, avoiding intricate time convolutions defining the inductions. In an absorptive spacetime, the complex dispersion relation rather than the choice of a residual integration path determines whether the Green function is retarded or advanced, cf. Sections 2 and 6.1. As transversal and longitudinal modes admit different dispersion relations, cf. Section 5.1, the Green functions for transversal and longitudinal propagation differ as well.

The dissipative tachyonic Cherenkov densities (7.6) determine the power measured at large distance from the radiating source. The radiation conditions for Cherenkov emission are the positivity of the generalized mass-squares $M_{T,L}^2$ in the dispersion relations, cf. (7.7), and the positivity of the argument $D_t^{T,L}$ in the Heaviside factor of the radiation densities (7.6). Condition $D_t^{T,L} \ge 0$ just means $\cos\theta_{T,L} \le 1$, where $\theta_{T,L}$ is the transversal/longitudinal Cherenkov angle, cf. after (7.4). The effect of the real part of the tachyon mass is evident in the mass-squares $M_{T,L}^2$, which remain positive even if the real parts of the permeabilities satisfy $\varepsilon_{Re}\mu_{Re} = 1$, $\varepsilon_{0,Re}\mu_{0,Re} = 1$, cf. after (8.2), in which case photonic Cherenkov radiation is forbidden.

To highlight the difference between photonic and tachyonic Cherenkov radiation further, we consider the transition from the classical to the quantum regime [26]. In the spectral fit of the supernova remnant, we used the classical spectral densities (7.6). The condition for the applicability of the classical densities is a small mass ratio $M_{T,L}^2(\omega)/m^2 \ll 1$, where $M_{T,L}^2$ are the transversal/longitudinal mass-squares (7.7) and m is the mass of the radiating electron; the quantum Cherenkov regime is realized in the opposite limit [26]. For photonic Cherenkov radiation, this condition simplifies to $\sqrt{\varepsilon_{Re}\mu_{Re} - 1}\,\omega/m \ll 1$, as the tachyonic mass term

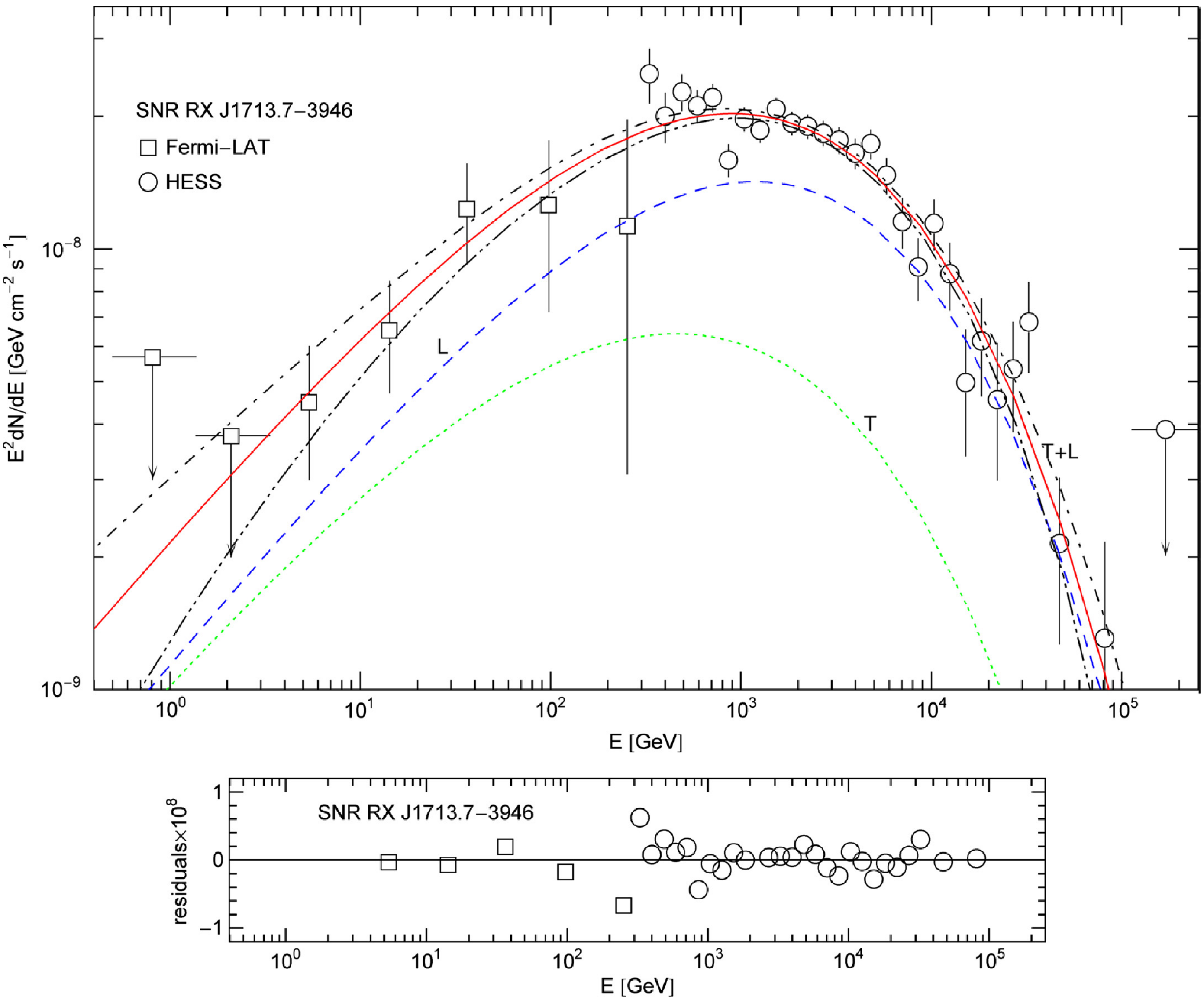

Fig. 1. Tachyonic γ-ray flux of supernova remnant RX J1713.7 − 3946, radiated by the shocked ultra-relativistic electron plasma. Data points from Fermi-LAT [10] and HESS [12]. The solid curve T + L depicts the unpolarized tachyonic energy flux $EF_E^{T+L} = E^2 dN^{T+L}/dE$, cf. (8.1) and (8.4), obtained by adding the transversal flux component EF_E^{T} (dotted curve, labeled T) to the longitudinal flux EF_E^{L} (dashed curve, L), cf. (8.2). The transversal radiation is linearly polarized. The error band defined by the dot-dashed curves indicates the upper and lower 1σ (68%) confidence limits of the least-squares fit (28 dof, $\chi^2 \approx 37.4$). The fine-structure scaling exponent $\sigma = \eta - 2\rho \approx -0.98$ is inferred from the scaling exponent of the tachyon mass, $\rho = 0.751 \pm 0.059$, and from the exponent $\eta = 0.520 \pm 0.17$ determining the slope of the initial power-law ascent of flux density (8.4). The fitting parameters are η, ρ, the Weibull decay exponent $\hat{\beta}[\mathrm{GeV}^{-1}] = 0.614 \pm 0.51$ and the flux amplitude $A_F[\mathrm{GeV\,cm^{-2}\,s^{-1}}] = (5.83 \pm 1.8) \times 10^{-10}$, cf. (8.4). The Weibull shape parameter determining the subexponential decay of the spectral tail is $1 - \rho \approx 0.25$. The mass scaling exponent ρ lies above 1/2, implying subluminal group velocity of the γ-rays, cf. the end of Section 8.

in M_T^2 vanishes, so that the energy of the radiated photons must be much smaller than the electron mass for the classical photonic spectral density (see after (7.5)) to apply. As pointed out after (7.8), positivity of the mass-squares $M_{T,L}^2(\omega)$ is a necessary condition for Cherenkov emission at the respective frequency, so that $\varepsilon_{\mathrm{Re}}\mu_{\mathrm{Re}} > 1$ is required in the photonic case, a refractive index exceeding one.

In contrast, a tachyonic Cherenkov density is employed in the spectral fit of the SNR shown in Fig. 1. Instead of dropping the tachyonic mass term in $M_{T,L}^2$, we consider permeabilities satisfying $\varepsilon_{\mathrm{Re}}\mu_{\mathrm{Re}} \sim \varepsilon_{0,\mathrm{Re}}\mu_{0,\mathrm{Re}} \sim 1$, so that the first term in the mass-squares (7.7) vanishes. The condition $M_{T,L}^2/m^2 \ll 1$ for the classical limit then amounts to a small tachyon-electron mass ratio $\hat{m}_{t,\mathrm{Re}}^2/m^2 \ll 1$. Thus, if this mass ratio is small and the real parts of the permeabilities are close to one, the classical spectral densities (7.6) can be used to calculate the energy flux, cf. (8.1) and (8.4), even if the energy of the radiated quanta (GeV and TeV γ-rays emanating from the remnant) exceeds the electron mass, in contrast to photonic radiation which requires $\omega/m \ll 1$ for the classical limit to apply. Another marked difference to photonic Cherenkov emission is the longitudinal radiation component, which can even overpower the transversal radiation, see Fig. 1. The emitted tachyonic quanta can be superluminal, depending on the scaling exponent of the tachyon mass, cf. the end of Section 8, whereas the radiating electron gas is subluminal. Electromagnetic radiation from superluminally rotating light spots and accelerated superluminal particles has been studied in Refs. [32,33].

The tachyon mass in Lagrangian (2.1) is complex like the permeabilities. In the Cherenkov densities (7.6) and the averaged energy flux (8.2), the imaginary parts of the permeabilities and the tachyon mass generate the attenuation factor $\exp(-2k_{T,L,\mathrm{Im}}(\omega)d)$, where $k_{T,L,\mathrm{Im}}$ is the imaginary part of the transversal/longitudinal wavenumber and d the radial distance of the detector from the localized radiation source. At a distance of a few kiloparsecs from a Galactic source, this exponential factor is still close to one, otherwise the signal would have dissipated away. For the attenuation length $1/(2k_{\mathrm{T,L,Im}})$ to be of the same order or larger than the source distance d, the imaginary parts of the permeabilities must be tiny. Linearization in the imaginary parts of the permeabilities and tachyon mass (starting with the dispersion relations defining the wavenumbers, cf. Section 5.2) is thus amply justified in the Cherenkov densities (7.6).

Apart from the attenuation factor quantifying the absorption by the aether, there emerges a second decay factor in the spectral flux densities (8.4), the Weibull exponential $\exp(-\hat{\beta}\omega^{1-\rho})$, where ρ is the frequency scaling exponent of the tachyon mass and $\hat{\beta}$ the decay exponent inversely proportional to the temperature of the radiating electron plasma. This decay factor results in subexponential ($0 < \rho < 1$) spectral tails as found in the γ-ray spectra of pulsars [9,26] and supernova remnants, cf. Fig. 1. Subexponential decay approximating power-law decay seems to be a common feature of γ-ray spectral tails and has also been detected by the AGILE satellite [34] in the MeV spectra of terrestrial γ-ray flashes [35,36] at thundercloud altitudes.

References

[1] V.L. Ginzburg, Phys. Usp. 39 (1996) 973.
[2] V.L. Ginzburg, Phys. Usp. 45 (2002) 341.
[3] G.N. Afanasiev, V.G. Kartavenko, J. Phys. D, Appl. Phys. 31 (1998) 2760.
[4] G.N. Afanasiev, V.G. Kartavenko, E.N. Magar, Physica B 269 (1999) 95.
[5] R. Tomaschitz, Physica A 307 (2002) 375.
[6] R. Tomaschitz, Physica A 320 (2003) 329.
[7] R. Tomaschitz, Appl. Phys. B 101 (2010) 143.
[8] R. Tomaschitz, Phys. Lett. A 377 (2013) 3247.
[9] R. Tomaschitz, Europhys. Lett. 106 (2014) 39001.
[10] Fermi-LAT Collaboration, Astrophys. J. 734 (2011) 28.
[11] HESS Collaboration, Astron. Astrophys. 464 (2007) 235.
[12] HESS Collaboration, Astron. Astrophys. 531 (2011) C1.
[13] G.N. Afanasiev, V.G. Kartavenko, Yu.P. Stepanovsky, J. Phys. D, Appl. Phys. 32 (1999) 2029.
[14] G.N. Afanasiev, V.M. Shilov, J. Phys. D, Appl. Phys. 33 (2000) 2931.
[15] Y.-D. Jung, Phys. Lett. A 378 (2014) 2176.
[16] Y.-D. Jung, Phys. Plasmas 18 (2011) 064503.
[17] D.-H. Ki, Y.-D. Jung, Europhys. Lett. 91 (2010) 65001.
[18] R. Tomaschitz, Europhys. Lett. 97 (2012) 39003.
[19] R. Tomaschitz, Phys. Lett. A 377 (2013) 945.
[20] R. Tomaschitz, Europhys. Lett. 102 (2013) 61002.
[21] R. Tomaschitz, Opt. Commun. 282 (2009) 1710.
[22] V.L. Ginzburg, The Propagation of Electromagnetic Waves in Plasmas, 2nd ed., Pergamon Press, Oxford, 1970.
[23] V.M. Agranovich, V.L. Ginzburg, Crystal Optics with Spatial Dispersion, and Excitons, 2nd ed., Springer, Berlin, 1984.
[24] Yu.S. Barash, V.L. Ginzburg, Sov. Phys. JETP 42 (1975) 602.
[25] Yu.S. Barash, V.L. Ginzburg, Sov. Phys. Usp. 19 (1976) 263.
[26] R. Tomaschitz, Phys. Lett. A 378 (2014) 2337.
[27] R. Tomaschitz, Europhys. Lett. 98 (2012) 19001.
[28] R. Tomaschitz, Chaos Solitons Fractals 9 (1998) 1199.
[29] R. Tomaschitz, Class. Quantum Gravity 18 (2001) 4395.
[30] R. Tomaschitz, Physica B 404 (2009) 1383.
[31] R. Tomaschitz, Eur. Phys. J. C 69 (2010) 241.
[32] B.M. Bolotovskii, A.V. Serov, Radiat. Phys. Chem. 75 (2006) 813.
[33] R.A. Treumann, Europhys. Lett. 16 (1991) 121.
[34] AGILE Collaboration, Phys. Rev. Lett. 106 (2011) 018501.
[35] J.R. Dwyer, M.A. Uman, Phys. Rep. 534 (2014) 147.
[36] S. Celestin, W. Xu, V.P. Pasko, J. Geophys. Res. 117 (2012) A05315.